

# Efficient Solid Emitters with Aggregation-Induced Emission and Intramolecular Charge Transfer Characteristics: Molecular Design, Synthesis, Photophysical Behaviors, and OLED Application

Wang Zhang Yuan,<sup>†,‡</sup> Yongyang Gong,<sup>‡</sup> Shuming Chen,<sup>§</sup> Xiao Yuan Shen,<sup>||</sup> Jacky W. Y. Lam,<sup>†</sup> Ping Lu,<sup>⊥</sup> Yawei Lu,<sup>‡</sup> Zhiming Wang,<sup>⊥</sup> Rongrong Hu,<sup>†</sup> Ni Xie,<sup>†</sup> Hoi Sing Kwok,<sup>§</sup> Yongming Zhang,<sup>‡</sup> Jing Zhi Sun,<sup>||</sup> and Ben Zhong Tang<sup>\*,†,||</sup>

<sup>†</sup>Department of Chemistry and State Key Laboratory of Molecular Neuroscience, Institute for Advanced Study, The Hong Kong University of Science & Technology (HKUST), Clear Water Bay, Kowloon, Hong Kong, China

<sup>‡</sup>School of Chemistry and Chemical Engineering, Shanghai Jiao Tong University, Shanghai 200240, China

<sup>§</sup>Center for Display Research, The Hong Kong University of Science & Technology (HKUST), Clear Water Bay, Kowloon, Hong Kong, China

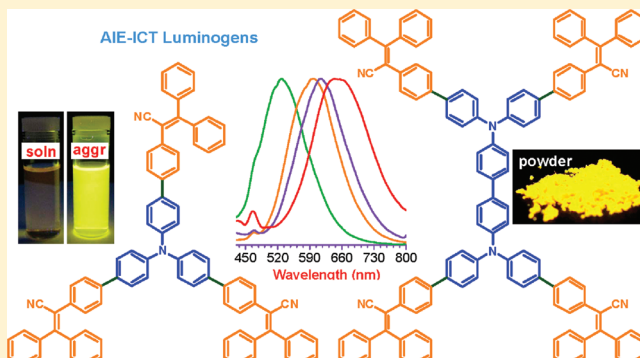
<sup>||</sup>Department of Polymer Science and Engineering, Zhejiang University, Hangzhou 310027, China

<sup>⊥</sup>State Key Laboratory of Supramolecular Structure and Materials, Jilin University, Changchun 130023, China

## Supporting Information

**ABSTRACT:** Emissive electron donor–acceptor (D–A) conjugates have a wide variety of applications in biophotonics, two-photon absorption materials, organic lasers, long wavelength emitters, and so forth. However, it is still a challenge to synthesize high solid-state efficiency D–A structured emitters due to the notorious aggregation-caused quenching (ACQ) effect. Though some D–A systems are reported to show aggregation-induced emission (AIE) behaviors, most are only selectively AIE-active in highly polar solvents, showing decreased solid-state emission efficiencies compared to those in nonpolar solvents. Here we report the triphenylamine (TPA) and 2,3,3-triphenylacrylonitrile (TPAN) based D–A architectures, namely, TPA3TPAN and DTPA4TPAN. Decoration of arylamines with TPAN changes their emission behaviors from ACQ to AIE, making resulting TPA3TPAN and DTPA4TPAN nonluminescent in common solvents but highly emissive when aggregated as nanoparticles, solid powders, and thin films owing to their highly twisted configurations. Both compounds also display a bathochromic effect due to their intramolecular charge transfer (ICT) attribute. Combined ICT and AIE features render TPA3TPAN and DTPA4TPAN intense solid yellow emitters with quantum efficiencies of 33.2% and 38.2%, respectively. They are also thermally and morphologically stable, with decomposition and glass transition temperatures ( $T_d/T_g$ ) being 365/127 and 377/141 °C, respectively. Multilayer electroluminescence (EL) devices are constructed, which emit yellow EL with maximum luminance, current, power, and external quantum efficiencies up to 3101 cd/m<sup>2</sup>, 6.16 cd/A, 2.64 lm/W, and 2.18%, respectively. These results indicate that it is promising to fabricate high efficiency AIE-ICT luminogens with tunable emissions through rational combination and modulation of propeller-like donors and/or acceptors, thus paving the way for their biophotonic and optoelectronic applications.

**KEYWORDS:** aggregation-induced emission, intramolecular charge transfer, high solid-state efficiency



## INTRODUCTION

Conjugated molecules with electron donor–acceptor (D–A) architectures are of growing interest for optoelectronic applications due to their unique photochemical and intramolecular charge transfer (ICT) properties.<sup>1–7</sup> The independent and diverse selections of donor and acceptor groups allow for facile modulation of the electronic structure and thus electronic and optoelectronic properties of the resulting conjugates, making them suitable for a wide variety of applications in solar energy conversion,<sup>5,8</sup> microenvironmental

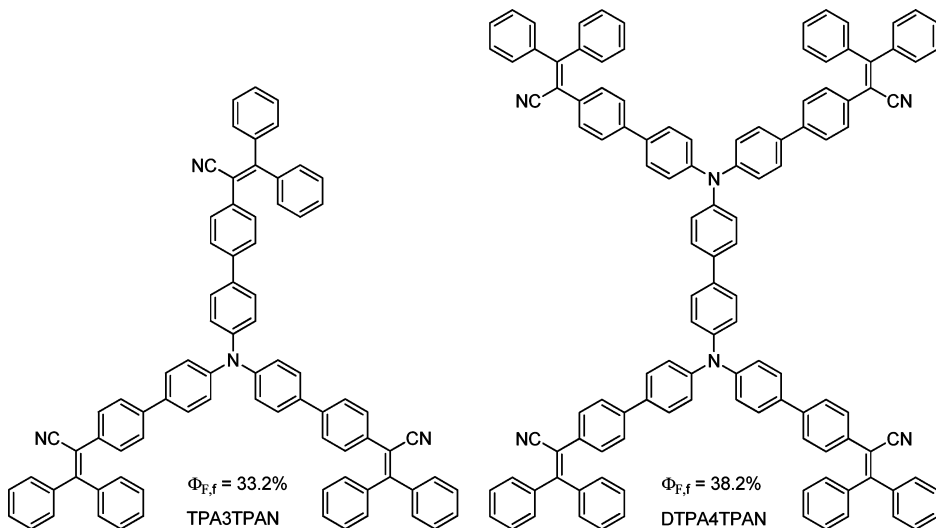
changes detection,<sup>9</sup> optoelectronic devices,<sup>5,7,10–12</sup> cellular imaging,<sup>13</sup> and so on. Particularly, emissive D–A conjugates are promising candidates for biophotonics and optoelectronics, such as fluorescent molecular rotors,<sup>14</sup> chemo- and bio-sensors,<sup>13b,15</sup> upconverting fluorophores,<sup>6b,c,16</sup> low band gap emitters,<sup>17</sup> organic lasers,<sup>18</sup> optical power limiting materials,<sup>19</sup>

**Received:** February 7, 2012

**Revised:** April 5, 2012

**Published:** April 6, 2012

Chart 1. Chemical Structures of TPA3TPAN and DTPA4TPAN



optical data storage media,<sup>20</sup> light-emitting diodes (LEDs),<sup>4,21</sup> and field-effect transistors (FETs).<sup>3d,22</sup>

Normally, strong fluorescence in the aggregated state is highly desired for most applications of emissive D–A conjugates, particularly for the biophotonic and electroluminescent cases.<sup>4,13a,21</sup> However, many conventional luminophores suffer from the notorious aggregation-caused quenching (ACQ) effect due to the formation of such detrimental species as excimers and exciplexes in the aggregated state.<sup>23,24</sup> Various chemical, physical, and engineering methods were exploited to prevent the formation of luminophore aggregates with the aim of mitigating the ACQ effect.<sup>25</sup> Such efforts, however, have met with only limited success, because they are basically working against a natural process: it is well-known that luminophore molecules inherently aggregate in the condensed phase. Contrary to the ACQ effect, we have recently discovered a novel phenomenon of aggregation-induced emission (AIE).<sup>26</sup> In sharp contrast to traditional luminophores, the AIE luminogens are nonemissive when dissolved in good solvents but become highly emissive upon aggregation in poor solvents or in the solid state.<sup>26–28</sup>

Meanwhile, traditional D–A structured luminogens are weakly or even nonemissive in highly polar solvents like DMF due to the presence of dark ICT state but normally exhibit high luminescence in nonpolar solvents (hexane, toluene, 1,4-dioxane, etc.) from the local excited (LE) state.<sup>3c,29</sup> This is the expected effect of ICT on solution quantum efficiency; namely, fluorescence efficiency should decrease with increasing charge transfer strength. The solid state emissions, however, depend on the molecular configurations despite the restricted ICT process: while distorted geometry diminishes the intermolecular interactions and thus favors efficient fluorescence,<sup>30,31</sup> planar structure induces strong  $\pi$ – $\pi$  interactions and thereby quenches the emission.<sup>29</sup>

Some works reported the D–A systems showing AIE characteristic in highly polar aqueous media. However, the solid-state efficiencies are still lower than those of molecularly dissolved species in nonpolar solvents;<sup>31</sup> namely, these molecules are only selectively AIE-active in specific solvents. Steady and transient absorption and emission studies revealed that the transition from emissive LE state to dark ICT state is the main cause for such selective AIE phenomena.<sup>31</sup>

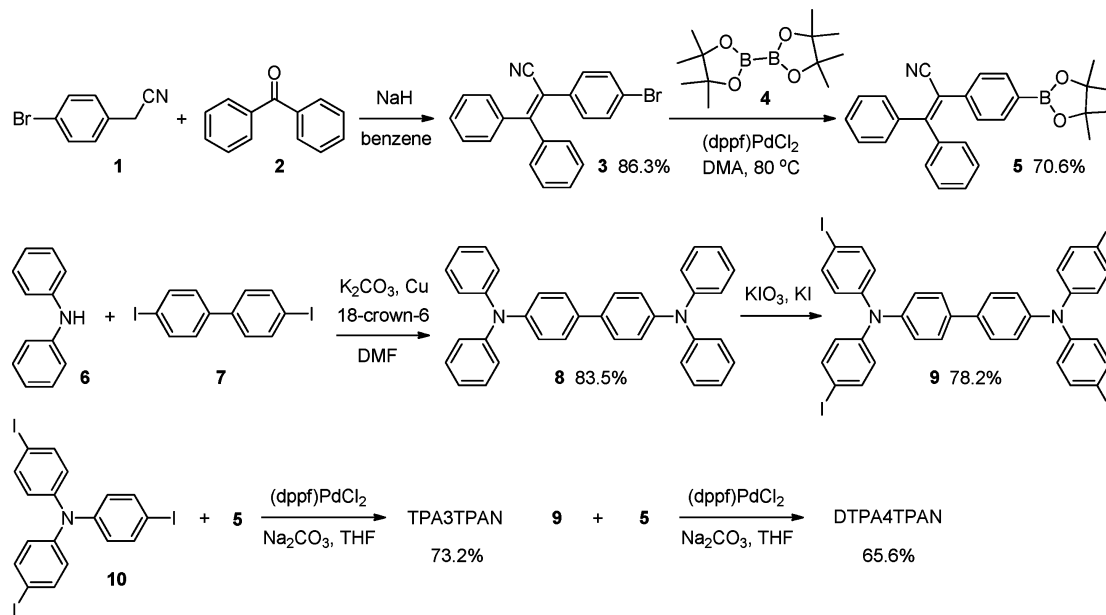
We are wondering whether we can create such D–A conjugates as normal AIE luminogens that are weakly or nonluminescent in common solvents but become strong emitters when aggregated. If so, it will be instructive to fabricate such highly fluorescent solid emitters as red and near-IR luminogens with tunable emissions, which have important applications in optoelectronic devices and biophotonics.<sup>32</sup> In the present paper, we endeavored to develop such D–A systems consisting of electron-donating triphenylamine (TPA) or  $N^4,N^4,N^4,N^4$ -tetraphenylbiphenyl-4,4'-diamine (a TPA dimer, DTPA) cores and electron-accepting 2,3,3-triphenylacrylonitrile (TPAN) peripherals, and the resulting TPA3TPAN and DTPA4TPAN (Chart 1) molecules exhibit typical AIE and ICT characteristics as expected.

## EXPERIMENTAL SECTION

**Materials.** THF and toluene were distilled under normal pressure from sodium benzophenone ketyl under nitrogen immediately prior to use. Dichloromethane (DCM) was distilled under normal pressure over calcium hydride under nitrogen before use. Benzene, dimethylformamide (DMF), dimethylacetamide (DMA), 4-bromobenzyl nitrile (**1**), benzophenone (**2**), sodium hydride (NaH), bis(pinacolato)diborane (**4**), 1,1'-bis(diphenylphosphino)ferrocene]-dichloropalladium(II) ((dppf)PdCl<sub>2</sub>), diphenylamine (**6**), 4,4'-diiodobiphenyl (**7**), potassium iodide (KI), potassium iodate (KIO<sub>3</sub>), and sodium carbonate (Na<sub>2</sub>CO<sub>3</sub>) were purchased from Aldrich and used as received. Tris(4-iodophenyl)amine (**10**) was synthesized according to reference procedures.<sup>33</sup>

**Instruments.** <sup>1</sup>H and <sup>13</sup>C NMR spectra were measured on a Bruker ARX 400 spectrometer using CDCl<sub>3</sub> as solvent and tetramethylsilane (TMS,  $\delta = 0$ ) as internal standard. Matrix-assisted laser desorption/ionization time-of-flight (MALDI-TOF) high-resolution mass spectra (HRMS) were recorded on a GCT premier CAB048 mass spectrometer. Absorption spectra were taken on a Milton Roy Spectronic 3000 Array spectrometer. Emission spectra were taken on a Perkin-Elmer spectrofluorometer LS 55. Emission quantum yields ( $\Phi_F$ 's) of TPA3TPAN and DTPA4TPAN in different solvents were estimated by using 9,10-diphenylanthracene ( $\Phi_F = 90\%$  in cyclohexane, for TPA3TPAN and DTPA4TPAN) or 2-amino pyridine ( $\Phi_F = 60\%$  in 0.1 N H<sub>2</sub>SO<sub>4</sub>, for TPAN) as standard, while solid-state efficiencies of the thin films were determined using an integrating sphere. Thermal stability of the compounds was evaluated on a Perkin-Elmer TGA 7 under nitrogen at a heating rate of 20 °C/min. A Perkin-Elmer DSC 7 was employed to measure the phase transition thermograms at a scan rate of 10 °C/min. The ground-state

Scheme 1. Synthetic Routes to TPA3TPAN and DTPA4TPAN



geometries were optimized using the density functional with B3LYP hybrid functional at the basis set level of 6-31G(d). All calculations were performed using the Gaussian 09 package. Cyclic voltammograms were recorded on a Zahner IM6e Electrochemical Workstation with Pt, glassy carbon, and Ag/AgCl electrodes as counter, working, and reference electrodes, respectively, at a scan rate of 100 mV/s, with 0.1 M tetrabutylammonium hexafluorophosphate ( $\text{Bu}_4\text{NPF}_6$ ) as the supporting electrolyte in anhydrous dichloromethane (DCM) purged with nitrogen. The HOMO energy levels are derived from the onset oxidation potentials ( $E_{\text{onset-ox}}$ ) according to the equation  $\text{HOMO} = -(E_{\text{onset-ox}} + 4.8 \text{ eV} - E_{\text{ferrocene}})$ . Optical band gaps ( $E_g^{\text{opt}}$ ) of the compounds were derived from the absorption edges in DCM, thereby giving the LUMO levels of  $(\text{HOMO} + E_g^{\text{opt}})$ .

**OLED Device Fabrication.** The devices were fabricated on an 80 nm-ITO coated glass with a sheet resistance of  $25 \Omega \square^{-1}$ . Prior to loading into the pretreatment chamber, the ITO-coated glass was soaked in ultrasonic detergent for 30 min, followed by spraying with deionized water for 10 min, soaking in ultrasonic deionized water for 30 min, and oven-baking for 1 h. The cleaned samples were treated by perfluoromethane plasma with a power of 100 W, gas flow of 50 sccm, and pressure of 0.2 Torr for 10 s in the pretreatment chamber. The samples were transferred to the organic chamber with a base pressure of  $7 \times 10^{-7}$  Torr for the deposition of 1,4-bis[(1-naphthylphenyl)-amino]biphenyl (NPB), emitter, and 1,3,5-tris(N-phenylbenzimidazol-2-yl)benzene (TPBi), which served as hole-transport, light-emitting, and electron-transport layers, respectively. The samples were then transferred to the metal chamber for cathode deposition to lithium fluoride (LiF) capped with aluminum (Al). The light-emitting area was 4 mm<sup>2</sup>. The current density–voltage characteristics of the devices were measured by a HP4145B semiconductor parameter analyzer. The forward direction photons emitted from the devices were detected by a calibrated UDT PIN-2SD silicon photodiode. The luminance and external quantum efficiencies of the devices were inferred from the photocurrent of the photodiode. The electroluminescence spectra were obtained by a PR650 spectrophotometer. All measurements were carried out under air at room temperature without device encapsulation. Due to the high molecular weight ( $M_w = 1606$ ) and dipole–dipole interactions, DTPA4TPAN needs high evaporation temperature (320–370 °C) to deposit, which might damage the molecules.

**Luminogen Preparation.** TPA-TPAN adducts were synthesized according to the synthetic routes shown in Scheme 1. Detailed synthetic procedures and characterization data are given in Supporting Information.

## RESULTS AND DISCUSSION

**Synthesis.** The synthetic routes to TPA3TPAN and DTPA4TPAN are depicted in Scheme 1. Briefly, the important intermediate 5 was synthesized by coupling between 4-bromobenzyl nitrile (1) and benzophenone (2), followed by metathesis of the bromine atom for boronpinacolate.<sup>34</sup> While 10 was prepared according to our previous procedures,<sup>33</sup> another key reactant 9 was obtained by Ullmann reaction between diphenylamine (6) and 4,4'-diiodobiphenyl (7) and then followed by iodination. Suzuki couplings of the aromatic boron reagent 5 with 10 and 9 catalyzed by (dppf)PdCl<sub>2</sub> in basic media give the desirable compounds of TPA3TPAN and DTPA4TPAN, respectively. All compounds were characterized by standard spectroscopic methods, from which satisfactory analysis data corresponding to their molecular structures were obtained (see Supporting Information for detail). The final products give  $[\text{M} + \text{H}]^+$  and  $\text{M}^+$  peaks at  $m/z$  1083.4620 (calcd: 1083.4427) and 1605.6542 (calcd: 1605.6478) in the HRMS spectra for TPA3TPAN and DTPA4TPAN (Figures S3 and S4, Supporting Information), confirming the formation of the expected adducts.

**Intramolecular Charge Transfer.** Combination of typical electron-donating TPA and electron-accepting cyano groups offers ready ICT process in TPA3TPAN and DTPA4TPAN. Since photophysics of the D–A conjugates in solutions are strongly dependent on the solvent polarity,<sup>29</sup> we thus examined the absorption and emission properties of both compounds in varying solvents.

As depicted in Figure 1A,B, both compounds exhibit two characteristic absorption bands in varying solvents, with shorter/longer-wavelength absorptions of ~318/390 and ~326/390 nm for TPA3TPAN and DTPA4TPAN, respectively, irrespective of the solvent polarity. The former band can be ascribed to the  $\pi-\pi^*$  transitions, whereas the latter is assignable to the ICT between electron rich arylamine and electron deficient cyano segments. Much longer  $\pi-\pi^*$  transition absorption wavelength of DTPA4TPAN than TPA3TPAN suggests its longer effective conjugation length.

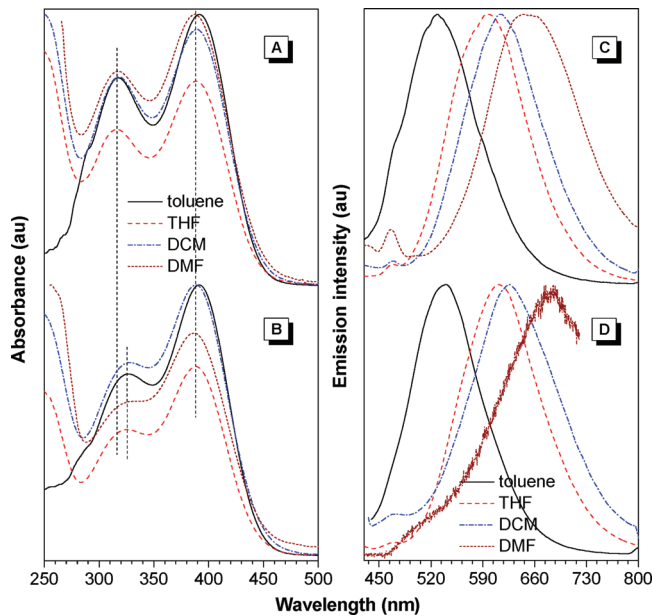


**Figure 1.** Normalized (A, B) absorption and (C, D) emission spectra of (A, C) TPA3TPAN and (B, D) DTPA4TPAN in varying solvents. Concentration = 5  $\mu$ M; excitation wavelength = 410 nm.

Their ICT absorptions, however, are similar due to almost identical electron donating and accepting strengths.

The absorption profile and maxima of both compounds are almost identical in varying solvents, suggesting their solvent polarity independent ground state electronic structures and small dipole moments associated with the ICT transitions. Additionally, the optical band gaps ( $E_g^{\text{opt}}$ ) deduced from the onset absorptions in DCM are 2.6 and 2.5 eV for TPA3TPAN and DTPA4TPAN, respectively, which are much narrower than those of 2.84 and 2.82 eV for their 3TPETPA and 4TPEDTPA congeners without cyano groups due to much stronger ICT effect.<sup>27b</sup>

Emission spectra of TPA3TPAN and DTPA4TPAN solutions are shown in Figure 1C,D. As the solvent polarity increased from nonpolar toluene to moderately polar THF and DCM and to highly polar DMF, the emission peaks are gradually red-shifted (also see Table 1), exhibiting an obvious bathochromic effect. The Stokes shifts ( $\Delta\nu$ ) of TPA3TPAN

**Table 1. Photophysical Properties of TPA3TPAN and DTPA4TPAN<sup>a</sup>**

solvent	$\Delta f$	$\lambda_{\text{ab}}$ (nm)	$\lambda_{\text{em}}$ (nm)	$\Delta\nu$ (cm <sup>-1</sup> )	$\Phi_{F,s}$ (%)
TPA3TPAN					
toluene	0.014	318, 392	529	6606.6	0.061
THF	0.210	316, 388	598	9050.8	0.225
DCM	0.218	318, 389	614	9420.3	0.232
DMF	0.275	317, 389	651	10346.0	0.041
DTPA4TPAN					
toluene	0.014	326, 391	540	7056.9	0.044
THF	0.210	325, 389	611	9340.3	0.478
DCM	0.218	328, 389	626	9732.5	0.003
DMF	0.275	329, 386	683	11265.4	0.014

<sup>a</sup>Abbreviation:  $\Delta f$  = solvent polarity parameters,  $\lambda_{\text{ab}}$  = absorption maximum,  $\lambda_{\text{em}}$  = emission maximum,  $\Phi_{F,s}$  = solution fluorescence quantum yield estimated by using 9,10-diphenylanthracen as standard ( $\Phi_F$  = 90% in cyclohexane).

and DTPA4TPAN in varying solvents were calculated, and their solvatochromic behaviors were quantitatively described by the Lippert–Mataga equation:<sup>35</sup>

$$\Delta\nu = \nu_a - \nu_e = \frac{2\Delta f}{hc\alpha^3}(\mu_E - \mu_G)^2 + \text{constant} \quad (1)$$

where  $\nu_a$  and  $\nu_e$  represent the maximum absorbance and emission wavenumbers,  $\mu_G$  and  $\mu_E$  are the dipole moments in the ground and excited states, and  $h$ ,  $c$ ,  $a$ , and  $n$  are the Planck constant, the speed of light, the Onsager solvent cavity radius, and the refractive index of the solvent, respectively.

The orientational polarizability,  $\Delta f$ , described in eq 2, is chosen as the measure of polarity.

$$\Delta f = \frac{\epsilon - 1}{2\epsilon + 1} - \frac{n^2 - 1}{2n^2 + 1} \quad (2)$$

where  $\epsilon$  is the static dielectric constant and  $n$  is the optical refractive index of the solvent.

The linear dependence of  $\Delta\nu$  on  $\Delta f$  together with the large slope of the  $\Delta\nu$  versus  $\Delta f$  plot (Figure 2) suggest that the ICT

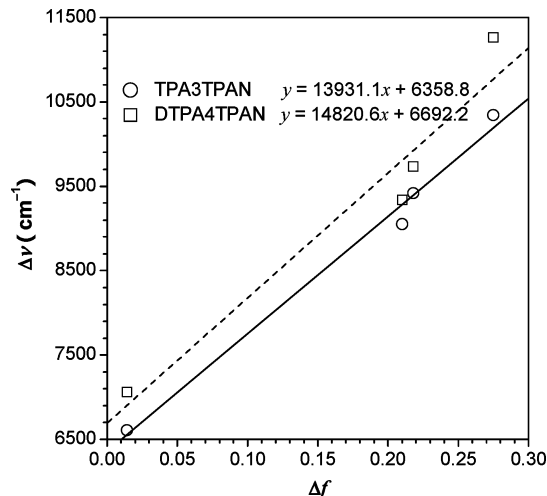


**Figure 2.** Plots of Stokes shift ( $\Delta\nu$ ) of TPA3TPAN and DTPA4TPAN vs solvent polarity parameter ( $\Delta f$ ).

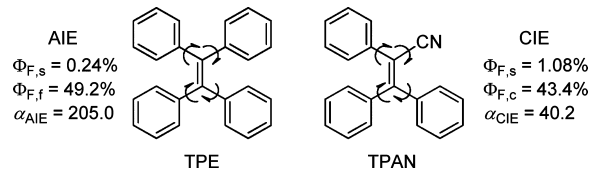
excited state has a larger dipolar moment than the ground state due to the substantial charge redistribution, which is probably derived from the relaxation of the initially formed Franck–Condon excited state, instead of the direct transition from the ground state. Meanwhile, according to Roncali and co-workers' work, a stronger ICT effect might be achieved if more powerful donor and acceptor moieties are adopted.<sup>5e,8d,e</sup>

The quantum efficiencies of the compounds in different solvents are also determined. As summarized in Table 1, neither of them emits effectively in solutions, which is similar to their 3TPETPA and 4TPEDTPA counterparts<sup>27b</sup> but distinctly different from traditional D–A structured molecules. Normally, D–A conjugates show weak or nonfluorescence in highly polar solvents due to the fast interconversion from the emissive local excited (LE) state to the low emissive ICT state; however, they exhibit much stronger emission in nonpolar solvents or in the solid state due to restricted ICT transitions.<sup>26,36</sup> Herein, TPA3TPAN and DTPA4TPAN are almost nonemissive in varying solvents, regardless of the solvent polarity. Such phenomenon should be ascribed to their strikingly twisted molecular configurations, which undergo active rotations and

vibrations in solutions, thus resulting in fast nonradiative relaxations and low emission quantum yields.<sup>26</sup>

**Aggregation-Induced Emission.** As discussed above, both TPA3TPAN and DTPA4TPAN are practically non-emissive when molecularly dissolved in solvents due to active intramolecular rotations and vibrations. It is known that TPE derivatives display AIE behaviors through a restricted intramolecular rotation (RIR) mechanism.<sup>26</sup> As a congener of TPE, TPAN (Chart 2) is nonemissive in solvents, amorphous

**Chart 2. Chemical Structures of TPE and TPAN**



nanosuspensions, and as a solid solution on TLC plate but highly fluorescent in the crystalline state (Figure S7, Supporting Information), exhibiting crystallization-induced emission (CIE) behaviors. The  $\Phi_F$  values of TPAN in THF and as crystalline powders are 1.08% and 43.4%, respectively, giving a CIE factor ( $\alpha_{CIE} = \Phi_{F,c}/\Phi_{F,s}$ ) of 40.2 (Chart 2). Therefore, TPAN decorated TPA3TPAN and DTPA4TPAN are expected to be AIE- or CIE-active. To check it, emission spectra of TPA3TPAN and DTPA4TPAN in THF and THF/water

aqueous media were conducted. Water is used because it is a nonsolvent for the compounds: the luminogens must aggregate in the aqueous mixtures with high water fractions ( $f_w$ ). As shown in Figure 3, the PL intensities of TPA3TPAN and DTPA4TPAN in THF are so low that only weak signals are recorded with maxima at 598 and 611 nm, respectively. With increasing  $f_w$ , the PL intensities initially decrease due to the increased solvent polarity<sup>37</sup> and then start to increase at the  $f_w$  of 50% and 40% for TPA3TPAN and DTPA4TPAN, respectively, at which solvating powers of the mixtures are worsened to such an extent that the luminogen molecules begin to aggregate. At a high  $f_w$  of 90%, nanoaggregates are formed, from which the PL peak intensities are increased by ~19- and ~14-fold when compared to their molecularly dispersed species in THF for TPA3TPAN and DTPA4TPAN, respectively, thus testifying to their AIE nature.

It is noticeable that both TPA and DTPA are ACQ chromophores, whose emission efficiencies in solution and thin film states are 13.0%/10.2% and 75.6%/13.7%, respectively.<sup>27b</sup> Decoration with TPAN changed their emission behaviors from ACQ to AIE, which is of crucial importance for the fabrication of high efficiency solid emitters.

Such an AIE attribute is also confirmed by the vivid image contrast of the luminogens in varying solvents and as solid powders. As depicted in Figure 4, neither TPA3TPAN nor DTPA4TPAN is emissive in toluene, THF, DCM, and DMF, but both emit intensely as aggregated solid powders. To quantitatively evaluate the AIE effect of the luminogens, the

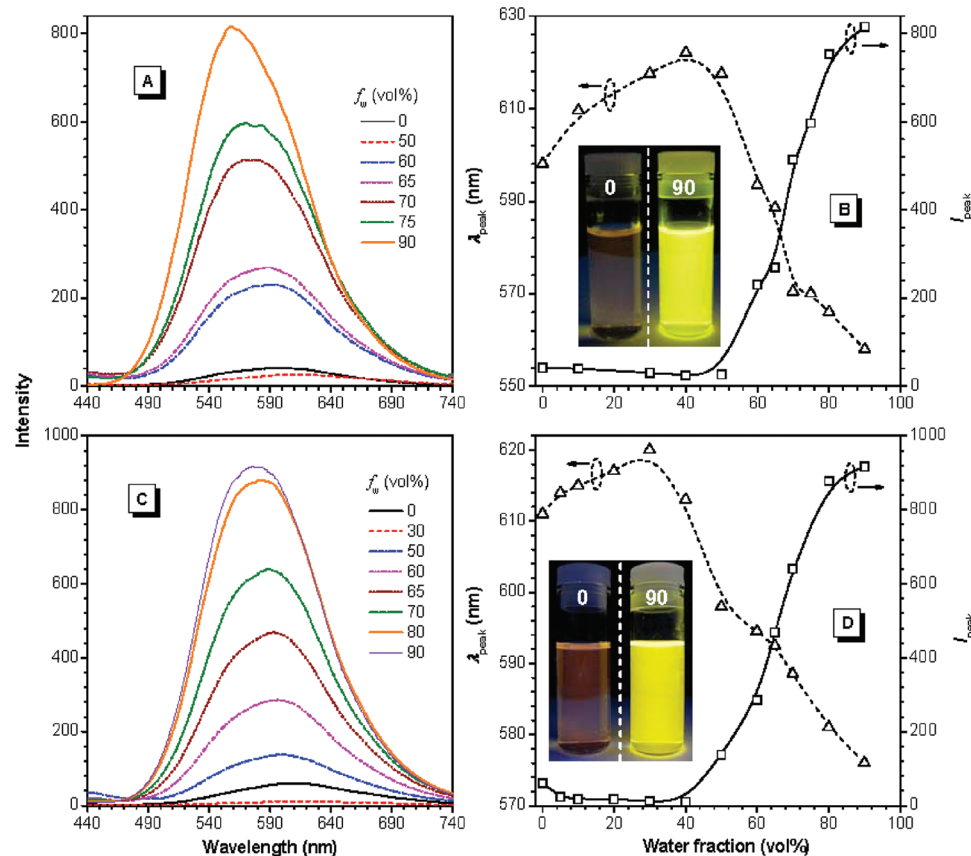


**Figure 3.** PL spectra of (A) TPA3TPAN and (C) DTPA4TPAN in THF and THF/water mixtures. Plots of PL peak location and intensity vs water fraction ( $f_w$ ) for (B) TPA3TPAN and (D) DTPA4TPAN. Concentration = 5  $\mu$ M; excitation wavelength = 380 nm. The inset graphs in (B) and (D) are the solutions of TPA3TPAN and DTPA4TPAN in THF ( $f_w = 0\%$ ) and their suspensions in THF/water mixture with  $f_w = 90\%$  under UV illumination.

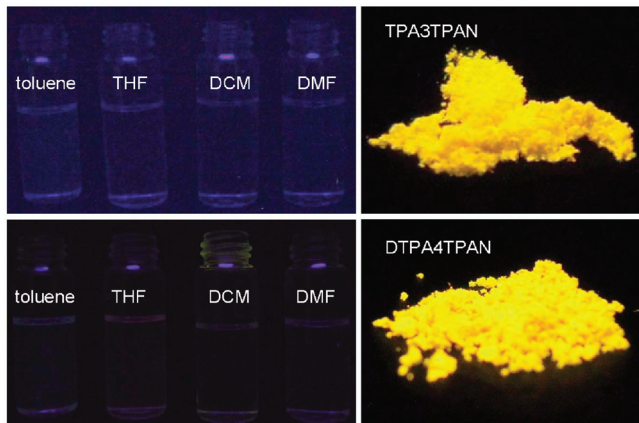


**Figure 4.** Photographs of (upper) TPA3TPAN and (lower) DTPA4TPAN in toluene, THF, DCM, and DMF and as solid powders under 365 nm UV light illumination.

thin-film emission spectra and quantum efficiencies ( $\Phi_{F,f}$ ) were determined. While TPA3TPAN displays a broad emission with the maximum at 563 nm, DTPA4TPAN exhibits the shoulder and peak emissions at 546 and 581 nm (Figure 5). The  $\Phi_{F,f}$

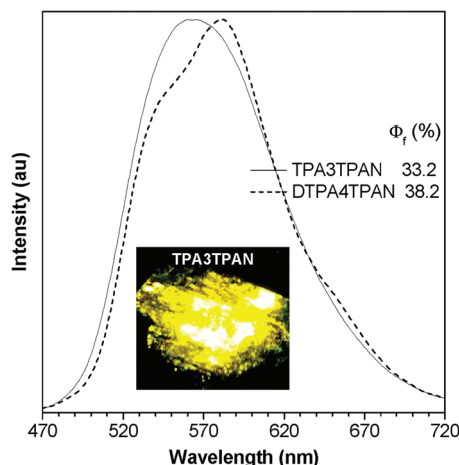


**Figure 5.** Film emission spectra of TPA3TPAN and DTPA4TPAN. Excitation wavelength = 390 nm. The inset graph is the TPA3TPAN thin film under 365 nm UV light illumination.

values are determined to be 33.2% and 38.2% for TPA3TPAN and DTPA4TPAN, respectively, which are considerably boosted compared to those in solutions, giving AIE factors ( $\alpha = \Phi_{F,f}/\Phi_{F,s}$ ) of 147.6 and 79.7 with respect to those in THF.

It is also noted that the emission peak varies with  $f_w$ . For example, with increasing  $f_w$ , the emission peak of TPA3TPAN is initially red-shifted until  $f_w$  reaches 40%, then remarkably blue-shifted, giving the emission peak from 598 to 622 nm, then to 558 nm when  $f_w$  is increased from 0 to 40%, and finally to 90% (Figure 3B). Such spectral shift can be explained as follows: when  $f_w$  is no more than 40%, TPA3TPAN molecules are still genuinely dissolved in the mixtures, and increasing  $f_w$  enhances the mixture polarity, consequently generating red-shifted emission due to the ICT effect; however, as  $f_w$  reaches 50%, owing to the decreased mixture solvating power, TPA3TPAN molecules start to aggregate, resulting in less polar microenvironment for the luminogens due to self-wrapping. The microenvironment gets less and less polar with more serious aggregation caused by increased  $f_w$ , thus

reversely giving blue-shifted emissions. DTPA4TPAN behaves similarly to TPA3TPAN. As shown in Figure 4B, when  $f_w$  is increased from 0 to 30% and then to 90%, the emission peak is first slightly red-shifted from 611 to 620 nm and then greatly blue-shifted to 576 nm.

To better understand the AIE nature of TPA3TPAN and DTPA4TPAN, quantum chemical optimization on their energy levels based on DFT/B3LYP/6-31G(d) using Gaussian 09 was conducted. The optimized geometries and HOMO/LUMO plots of TPA3TPAN and DTPA4TPAN are illustrated in Figure 6. Both molecules adopt highly twisted propeller-like

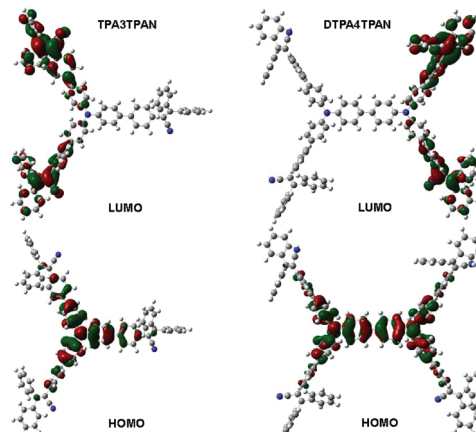


**Figure 6.** Optimized geometries and molecular orbital amplitude plots of HOMO and LUMO energy levels of TPA3TPAN and DTPA4TPAN.

nonplanar conformations, which are favorable for active intramolecular rotations of multiple phenyls and cyano groups in solutions, thereby powerfully dissipating the excitons energy and making them nonemissive in all solvents. Such emission behavior is strikingly different from that of conventional ICT systems, which are normally nonfluorescent in highly polar solvents but intensely emissive in nonpolar solvents. When aggregated as nanosuspensions, solid powders, or thin films, on one hand, the intramolecular rotations are impeded; on the other hand, the propeller-like configurations prevent the formation of detrimental excimers or exciplexes, thus endowing the aggregates with intense emission. Meanwhile, in polar solvents such as THF, DCM, and DMF, aggregation also partially restrains the ICT process, which is also helpful for the light emission.

Notably, the electron clouds of the HOMO levels for both luminogens are mainly located on the electron-donating TPA and DTPA units; however, those of LUMO levels are dominated by orbitals from the electron-accepting TPAN peripheries. Generally, such electron distribution imparts the dye molecules with an intrinsic intramolecular charge transfer property, which is consistent with the experimental data. Meanwhile, despite different molecular structures and HOMO levels, TPA3TPAN and DTPA4TPAN have almost identical LUMO levels with electron clouds distributed on two TPAN units connecting with one TPA moiety, indicative that their differences in ICT property inherently lies in the electron donor segments.

**Electrochemical Property.** Electrochemical properties of TPA3TPAN and DTPA4TPAN are investigated by cyclic voltammetry in 0.1 M solution of  $(Bu_4N)PF_6$  in DCM with a

glassy carbon electrode as the working electrode. As shown in Figure 7, both compounds show reversible *p*-doping processes.

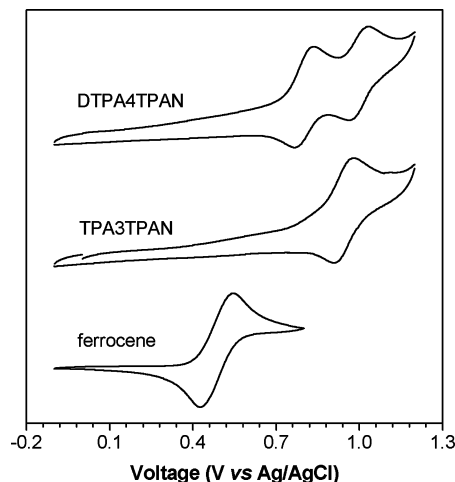


**Figure 7.** Cyclic voltammograms of TPA3TPAN and DTPA4TPAN in DCM with 0.1 M  $\text{Bu}_4\text{NPF}_6$  as a supporting electrolyte at a scan rate of 100 mV/s.

While TPA3TPAN exhibits only one oxidation peak, DTPA4TPAN shows two peaks associated to the formation of radical cations and dications. The onset oxidation potentials ( $E_{\text{onset-ox}}$ ) for TPA3TPAN, DTPA4TPAN, and ferrocene are 0.75, 0.66, and 0.33 eV, giving corresponding HOMO levels for the luminogens of  $-5.2$  and  $-5.1$  eV, respectively. The slightly lower  $E_{\text{onset-ox}}$  of DTPA4TPAN compared to TPA3TPAN is presumably due to the more extensively delocalized HOMO structure (Figure 6). Together with the optical band gaps ( $E_g^{\text{opt}}$ ) deduced from the onset absorptions in DCM, the same LUMO energy levels of  $-2.6$  eV are derived for both luminogens, which is in good agreement with the above calculation result.

**Thermal Properties.** Excellent thermal stability is highly desired for the device fabrication and optoelectronic applications for molecular conjugates. Particularly,  $T_g$  of an organic luminophore is one of the most important factors influencing the device stability and lifetime.<sup>38</sup> Once a device is heated above  $T_g$  of the organic luminophores, irreversible failure can occur. Therefore, we checked the thermal property of TPA3TPAN and DTPA4TPAN by thermogravimetric analysis (TGA) and differential scanning calorimetry (DSC) measurements. As shown in Figure 8, both TPA3TPAN and DTPA4TPAN enjoy high thermal stability with  $T_d$  (defined as the temperature at which a sample loses its 5% weight) values of 365 and 377 °C, respectively. DSC analysis reveals the  $T_g$ 's for TPA3TPAN and DTPA4TPAN are 127 and 141 °C, respectively, indicating excellent morphological stability of both compounds. Coupled with their efficient solid-state emissions, the dye molecules thus are promising candidates for such optoelectronic applications as EL emitters.

**Electroluminescence.** The high solid-state emission efficiency and good thermal and morphological stability of TPA3TPAN and DTPA4TPAN promoted us to investigate their EL performances. We first constructed a typical three-layer EL device with the configuration of ITO/NPB (60 nm)/TPA3TPAN (20 nm)/TPBi (40 nm)/LiF (1 nm)/Al (100 nm) (device I) using TPA3TPAN as a light-emitting layer (LEL). As illustrated in Figure 9, the device is turned on at 8.9

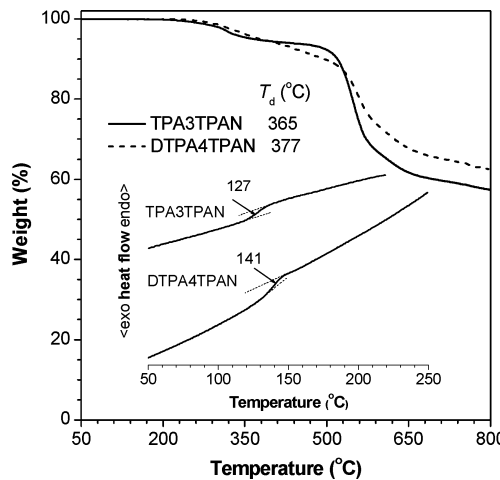


**Figure 8.** TGA and DSC (inset) thermograms of TPA3TPAN and DTPA4TPAN recorded under nitrogen at the scan rates of 20 and 10 °C/min, respectively.

$V_v$  emits at 556 and 575 nm, and exhibits maximum luminance ( $L_{\text{max}}$ ), current, power, and external quantum efficiencies ( $\text{CE}_{\text{max}}$   $\text{PE}_{\text{max}}$  EQE) of 1867 cd/m<sup>2</sup>, 2.45 cd/A, 0.48 lm/W, and 0.79%, respectively. Though the result is fair, it already demonstrates the potential applications of TPA3TPAN in OLEDs. Since the cyano group is a strong electron withdrawing group, it is suspected that TPA3TPAN may have good electron-transporting property. Therefore, we fabricated a double-layer EL devices without electron-transporting TPBi with the configuration of ITO/NPB (60 nm)/TPA3TPAN (60 nm)/LiF (1 nm)/Al (100 nm) (device II). While the EL spectrum profile of the device is almost identical to that of device I (Figure 9A), its performance gets even worse with the turn-on voltage ( $V_{\text{on}}$ ),  $L_{\text{max}}$   $\text{CE}_{\text{max}}$   $\text{PE}_{\text{max}}$  and EQE being 8.0 V, 572 cd/m<sup>2</sup>, 0.35 cd/A, 0.12 lm/W, and 0.13%, respectively. It is understandable that the device without the TPBi layer is not efficient because of quenching at the cathode. The result strongly suggests that an additional electron-transporting layer is beneficial to the device performance of TPA3TPAN, though electron deficient cyano groups are incorporated.

TPA derivatives are well-known hole-transporting materials.<sup>39</sup> Our previous studies have shown that TPA-containing AIE luminogens exhibit excellent hole-transporting property, whose EL devices without the hole-transporting NPB layer perform even better than those with.<sup>27b,40</sup> To improve the device performance, we thus newly fabricated a device without NPB with a configuration of ITO/TPA3TPAN (80 nm)/TPBi (40 nm)/LiF (1 nm)/Al (100 nm) (device III). The EL results are displayed in Figure 9 and are summarized in Table 2. Apparently, device III performs best, whose maximal luminance and efficiencies are remarkably improved when compared to devices I and II, giving  $L_{\text{max}}$   $\text{CE}_{\text{max}}$   $\text{PE}_{\text{max}}$  and EQE of 3101 cd/m<sup>2</sup>, 6.16 cd/A, 2.64 lm/W, and 2.78%, respectively. Such good result indicates that TPA3TPAN is not only a good EL emitter but also an excellent hole-transporting material. The use of NPB as an additional hole-transporting layer is thus not necessary and could be even harmful because it increases the contact impedance and also may break the charge balance in the EL device.

Herein, without an additional NPB layer, the contact resistance and energy barrier are lowered (Figure S8, Supporting Information). Moreover, excessive hole-injection

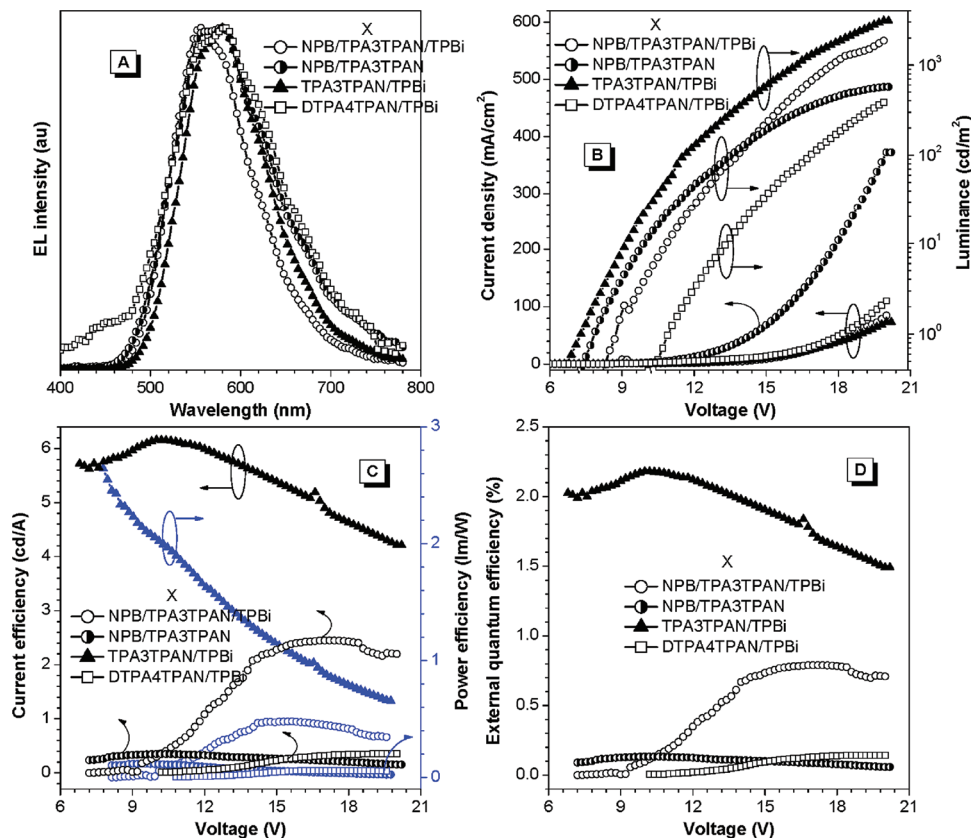


**Figure 9.** (A) EL spectra of TPA3TPAN and DTPA4TPAN, (B) current density–voltage–luminance plots, (C) current efficiency–voltage–power efficiency plots, and (D) external quantum efficiency–voltage plots of their multilayer LEDs with a general device configuration of ITO/X/LiF/Al.

**Table 2. Performance of the EL Devices of TPA3TPAN and DTPA4TPAN<sup>a</sup>**

device	$\lambda_{\max}$ (nm)	$V_{on}$ (V)	$L_{\max}$ (cd/m <sup>2</sup> )	$PE_{\max}$ (lm/W)	$CE_{\max}$ (cd/A)	EQE (%)
I	556, 575	8.9	1867	0.48	2.45	0.79
II	561, 579	8.0	572	0.12	0.35	0.13
III	580	7.4	3101	2.64	6.16	2.18
IV	558, 582	11.0	387	0.06	0.35	0.14

<sup>a</sup>Device configuration: ITO/X/LiF (1 nm)/Al (100 nm); X = NPB (60 nm)/TPA3TPAN (20 nm)/TPBi (40 nm) (device I), NPB (60 nm)/TPA3TPAN (60 nm) (device II), TPA3TPAN (80 nm)/TPBi (40 nm) (device III), DTPA4TPAN (20 nm)/TPBi (40 nm) (device IV); abbreviations:  $\lambda$  = EL peak,  $V_{on}$  = turn on voltage,  $L_{\max}$  = maximum luminance,  $PE_{\max}$  = maximum power efficiency,  $CE_{\max}$  = maximum current efficiency, and EQE = maximum external quantum efficiency.

is eliminated to reach a much better charge balance in the emitting layers, thus giving excellent EL performance. Therefore, TPA3TPAN can serve as an emissive component as well as hole-transport material in the EL devices. The multifunctional property of TPA3TPAN helps to simplify the device structure, shorten the fabrication process, reduce the production cost, and moreover enhance the device performance.<sup>21a,27b,41</sup> It is also notable that the EL devices of TPA3TPAN are unoptimized; thus, much better performance including the brightness and efficiency could be achieved through further optimizations as interlayer and anode modifications, tuning drift mobility, charge balance, and other engineering efforts.<sup>42</sup>

As an analogue of TPA3TPAN, DTPA4TPAN may have similar optoelectronic properties; we thus fabricated device IV using DTPA4TPAN as the emitting layer without NPB with the architecture of ITO/DTPA4TPAN (20 nm)/TPBi (40 nm)/LiF (1 nm)/Al (100 nm). The EL spectrum of device IV peaks at 558 and 582 nm. However, the device performance is far from ideal; the  $CE_{\max}$ ,  $PE_{\max}$ , and EQE are merely 0.35 cd/A, 0.06 lm/W, and 0.14%, respectively, presumably caused by the high evaporation temperature induced destruction of DTPA4TPAN (high evaporation temperature of 320–370 °C). Notably, DTPA4TPAN shows good film-forming ability; thus, its solution casting OLED devices may achieve better performances. And we will try such solution processable molecular devices in future.

## CONCLUSIONS

A combination of electron-donating arylamines (TPA, DTPA) and electron-accepting TPAN with propeller-like configurations yields TPA3TPAN and DTPA4TPAN with typical D–A architectures. Both compounds show bathochromic shift in varying solvents due to the ICT effect. Moreover, decoration of TPA and DTPA with TPAN changed their emission behaviors from ACQ to AIE: while TPA and DTPA are subject to an ACQ problem in the solid state, the resulting TPA3TPAN and DTPA4TPAN are practically nonluminescent when molecularly dissolved in solvents but emit intensely upon aggregate formation, demonstrating a typical AIE feature. Owing to the combined ICT and AIE attributes, their nanoaggregates, solid powders, and thin films emit yellow light intensely, with the thin film quantum efficiencies of 33.2% and 38.2% for TPA3TPAN and DTPA4TPAN, respectively. Both luminogens

enjoy high thermal stability ( $T_d \geq 365$  °C) and are morphologically stable ( $T_g \geq 127$  °C). An unoptimized EL device with the configuration of ITO/TPA3TPAN/TPBi/LiF/Al is constructed, which gives efficient yellow EL with maximum luminance and efficiencies of 3101 cd/m<sup>2</sup>, 6.16 cd/A, 2.64 lm/W, and 2.18%.

Unlike traditional D–A structured ICT systems, which are either subjected to a serious ACQ problem or only selectively AIE-active in highly polar solvents, TPA3TPAN and DTPA4TPAN exhibit typical AIE behaviors in all solvents. The present results indicate that the combination of electron donors and propeller TPAN acceptors is a promising approach to generate AIE-ICT luminogens with efficient solid emissions and tunable emission colors. Further modulation of the donor and acceptor strengths is expected to generate more AIE luminogens with tunable emissions and multifunctional properties.

## ASSOCIATED CONTENT

### Supporting Information

Synthetic procedures and characterization data, HRMS spectra of important intermediates (5 and 9), TPA3TPAN, and DTPA4TPAN, absorption and emission spectra of TPA, DTPA, and TPAN, emission spectra of TPAN in THF and THF/water aqueous mixtures, photographs and XRD pattern of TPAN, time-resolved fluorescence plots, and energy level diagrams of the EL devices (PDF). This material is available free of charge via the Internet at <http://pubs.acs.org>.

## AUTHOR INFORMATION

### Corresponding Author

\*E-mail: tangbenz@ust.hk. Phone: +852-2358-7375. Fax: +852-2358-1594.

### Notes

The authors declare no competing financial interest.

## ACKNOWLEDGMENTS

The work reported in this paper was partially supported by the National Science Foundation of China (21104044, 20974028), the RPC and SRFI Grants of HKUST (RPC10SC13, RPC11SC09, and SRFI11SC03PG), the Research Grants Council of Hong Kong (604711, 603509, HKUST2/CRF/10, and N\_HKUST620/11), the Innovation and Technology Commission (ITCPD/17-9), and the University Grants Committee of Hong Kong (AoE/P-03/08 and T23-713/11-1). B.Z.T. thanks the support from the Cao Guangbiao Foundation of Zhejiang University. W.Z.Y. thanks the support from Ph.D. Programs Foundation of Ministry of Education of China (20110073120040) and the Start-up Foundation for New Faculties of Shanghai Jiao Tong University.

## REFERENCES

- (1) (a) Bryce, M. R. *Adv. Mater.* **1999**, *11*, 11. (b) Grabowski, Z. R.; Rotkiewicz, K. *Chem. Rev.* **2003**, *103*, 3899.
- (2) (a) Wu, P.-T.; Kim, F. S.; Jenekhe, S. A. *Chem. Mater.* **2011**, *23*, 4618. (b) Ahmed, E.; Subramaniyan, S.; Kim, F. S.; Xin, H.; Jenekhe, S. A. *Macromolecules* **2011**, *44*, 7207. (c) Kim, F. S.; Guo, X.; Watson, M. D.; Jenekhe, S. A. *Adv. Mater.* **2010**, *22*, 478.
- (3) (a) Ahmed, J. E.; Ren, G.; Kim, F. S.; Emily C. Hollenbeck, E. C.; Jenekhe, S. A. *Chem. Mater.* **2011**, *23*, 4563. (b) Ellinger, S.; Graham, K. R.; Shi, P.; Farley, R. T.; Steckler, T. T.; Brookins, R. N.; Taranekar, P.; Mei, J.; Padilha, L. A.; Ensley, T. R.; Hu, H.; Webster, S.; Hagan, D. J.; Van Stryland, E. W.; Schanze, K. S.; Reynolds, J. R. *Chem. Mater.* **2011**, *23*, 3805. (c) Jenekhe, S. A.; Lu, L.; Alam, M. M. *Macromolecules* **2001**, *34*, 7315. (d) Zhu, Y.; Champion, R. D.; Samson, A. *Macromolecules* **2006**, *39*, 8712.
- (4) (a) Shirota, Y. *J. Mater. Chem.* **2005**, *15*, 75. (b) Justin Thomas, K. R.; Lin, J. T.; Tao, Y.-T.; Chuen, C.-H. *Chem. Mater.* **2004**, *16*, 5437. (c) Thomas, K. R.; Lin, J. R.; Velusamy, M.; Tao, Y.-T.; Chuen, C.-H. *Adv. Funct. Mater.* **2004**, *14*, 83.
- (5) (a) Cremer, J.; Bäuerle, P. *J. Mater. Chem.* **2006**, *16*, 874. (b) Roquet, S.; Cravino, A.; Leriche, P.; Alévéque, O.; Frère, P.; Roncali, J. *J. Am. Chem. Soc.* **2006**, *128*, 3459. (c) Esteban, S. G.; de la Cruz, P.; Aljarilla, A.; Arellano, L. M.; Langa, F. *Org. Lett.* **2011**, *13*, 5362. (d) Lin, L.-Y.; Chen, Y.-H.; Huang, Z.-Y.; Lin, H.-W.; Chou, S.-H.; Lin, F.; Chen, C.-W.; Liu, Y.-H.; Wong, K.-T. *J. Am. Chem. Soc.* **2011**, *133*, 15822. (e) Roncali, J. *Adv. Energy Mater.* **2011**, *1*, 147. (f) Zhang, X.; Shim, J. W.; Tiwari, S. P.; Zhang, Q.; Norton, J. E.; Wu, P.-T.; Barlow, S.; Jenekhe, S. A.; Kippelen, B.; Brédas, J.-L.; Marder, S. R. *J. Mater. Chem.* **2011**, *21*, 4971.
- (6) (a) Noh, S. B.; Kim, R. H.; Kim, W. J.; Kim, S.; Lee, K.-S.; Cho, N. S.; Shim, H.-K.; Pudavar, H. E.; Prasad, P. N. *J. Mater. Chem.* **2010**, *20*, 7422. (b) Jiang, Y.; Wang, Y.; Hua, J.; Tang, J.; Li, B.; Qian, S.; Tian, H. *Chem. Commun.* **2010**, *46*, 4689. (c) Wang, B.; Wang, Y.; Hua, J.; Jiang, Y.; Huang, J.; Qian, S.; Tian, H. *Chem.—Eur. J.* **2011**, *17*, 2647.
- (7) (a) He, G. S.; Xu, G. C.; Prasad, P. N.; Reinhardt, B. A.; Bhatt, J. C.; Dillard, A. G. *Opt. Lett.* **1995**, *20*, 435. (b) Lin, T.-C.; He, G. S.; Zheng, Q.; Prasad, P. N. *J. Mater. Chem.* **2006**, *16*, 2490.
- (8) (a) Blouin, N.; Michaud, M.; Gendron, D.; Wakim, S.; Blair, E.; Neagu-Plesu, R.; Belletête, M.; Durocher, G.; Tao, Y.; Leclerc, M. *J. Am. Chem. Soc.* **2008**, *130*, 732. (b) Zhang, Q.; Tour, J. M. *J. Am. Chem. Soc.* **1998**, *120*, 5355. (c) Ajayaghosh, A. *Chem. Soc. Rev.* **2003**, *32*, 181. (d) Cravino, A.; Leriche, P.; Alévéque, O.; Roquet, S.; Roncali, J. *Adv. Mater.* **2006**, *18*, 3033. (e) Roquet, S.; Cravino, A.; Leriche, P.; Alévéque, O.; Frère, P.; Roncali, J. *J. Am. Chem. Soc.* **2006**, *128*, 3459.
- (9) (a) Mallick, A.; Haldar, B.; Chattopadhyay, N. *J. Phys. Chem. B* **2005**, *109*, 14683. (b) Singh, R. B.; Mahanta, S.; Guchhait, N. *Spectrochim. Acta, Part A* **2009**, *72*, 1103.
- (10) (a) Thompson, B. C.; Frechet, J. M. *J. Angew. Chem., Int. Ed.* **2008**, *47*, 58. (b) Cheng, Y.-J.; Yang, S.-H.; Hsu, C.-S. *Chem. Rev.* **2009**, *109*, 5868. (c) Kim, F. S.; Ren, G.; Jenekhe, S. A. *Chem. Mater.* **2011**, *23*, 682. (d) Osaka, I.; Sauve, G.; Zhang, R.; Kowalewski, T.; McCullough, R. D. *Adv. Mater.* **2007**, *19*, 4160. (e) Osaka, I.; Takimiya, K.; McCullough, R. D. *Adv. Mater.* **2010**, *22*, 4993.
- (11) (a) Peumans, P.; Forrest, S. R. *Appl. Phys. Lett.* **2001**, *79*, 126. (b) Peumans, P.; Yakimov, A.; Forrest, S. R. *J. Appl. Phys.* **2003**, *93*, 3693. (c) Roquet, S.; Cravino, A.; Leriche, P.; Aleveque, O.; Frere, P.; Roncali, J. *J. Am. Chem. Soc.* **2006**, *128*, 3459.
- (12) (a) Belfield, K. D.; Liu, Y.; Negres, R. A.; Fan, M.; Pan, G.; Hagan, D. J.; Hernandez, F. E. *Chem. Mater.* **2002**, *14*, 3663. (b) Bhawalkar, J. D.; He, G. S.; Park, C. K.; Zhao, C. F.; Ruland, G.; Prasad, P. N. *Opt. Commun.* **1996**, *124*, 33. (c) He, G. S.; Helgeson, R.; Lin, T. C.; Zheng, Q.; Wudl, F.; Prasad, P. N. *IEEE J. Quantum Electron.* **2003**, *39*, 1003. (d) He, G. S.; Bhawalkar, J. D.; Zhao, C. F.; Prasad, P. N. *Appl. Phys. Lett.* **1995**, *67*, 2433.
- (13) (a) Kim, E.; Park, S. B. *Chem. Asian J.* **2009**, *4*, 1646. (b) Qian, F.; Zhang, C.; Zhang, Y.; He, W.; Gao, X.; Hu, P.; Guo, Z. *J. Am. Chem. Soc.* **2009**, *131*, 1460.
- (14) (a) Benjelloun, A.; Brembilla, A.; Lochon, P.; Adibnejad, M.; Viriot, M.-L.; Carré, M.-C. *Polymer* **1996**, *37*, 879. (b) Demchenko, A. P.; Mély, Y.; Duportail, G.; Klymchenko, A. S. *Biophys. J.* **2009**, *96*, 3461.
- (15) (a) Sauer, M. *Angew. Chem., Int. Ed.* **2003**, *42*, 1790. (b) Wilson, J. N.; Bunz, U. H. F. *J. Am. Chem. Soc.* **2005**, *127*, 4124. (c) Aoki, S.; Kagata, D.; Shiro, M.; Takeda, K.; Kimura, E. *J. Am. Chem. Soc.* **2004**, *126*, 13377. (d) Suzuki, Y.; Yokoyama, K. *J. Am. Chem. Soc.* **2005**, *127*, 17799. (e) Das, R.; Guha, D.; Mitra, S.; Kar, S.; Lahiri, S.; Mukherjee, S. *J. Phys. Chem. A* **1997**, *101*, 4042. (f) Valeura, B.; Leraya, I. *Coord. Chem. Rev.* **2000**, *205*, 3.

- (16) (a) Fang, H. H.; Chen, Q. D.; Yang, J.; Xia, H.; Gao, B. R.; Feng, J.; Ma, Y.; Sun, H. B. *J. Phys. Chem. C* **2010**, *114*, 11958. (b) Fang, H. H.; Chen, Q. D.; Yang, J.; Xia, H.; Ma, Y.; Wang, H. Y.; Sun, H. B. *Opt. Lett.* **2010**, *35*, 441. (c) Kim, S.; Zheng, Q.; He, G. S.; Bharali, D. J.; Pudavar, H. E.; Baev, A.; Prasad, P. N. *Adv. Funct. Mater.* **2006**, *16*, 2317.
- (17) (a) Qian, G.; Zhong, Z.; Luo, M.; Yu, D.; Zhang, Z.; Wang, Z. Y.; Ma, D. *Adv. Mater.* **2009**, *21*, 111. (b) Velusamy, M.; Justin Thomas, K. R.; Lin, J. T.; Wen, Y. S. *Tetrahedron Lett.* **2005**, *46*, 7647. (c) Kato, S.; Matsumoto, T.; Ishii, T.; Thiemann, T.; Shigeiwa, M.; Gorohmaru, H.; Maeda, S.; Yamashita, Y.; Mataka, S. *Chem. Commun.* **2004**, 2342.
- (18) (a) Chen, Q. D.; Fang, H. H.; Xu, B.; Yang, J.; Xia, H.; Chen, F. P.; Tian, W. J.; Sun, H. B. *Appl. Phys. Lett.* **2009**, *94*, 201113. (b) He, G. S.; Lin, T. C.; Hsiao, V. K. S.; Cartwright, A. N.; Prasad, P. N.; Natarajan, L. V.; Tondiglia, V. P.; Jakubiak, R.; Vaia, R. A.; Bunning, T. *J. Appl. Phys. Lett.* **2003**, *83*, 2733. (c) Tang, X. J.; Wu, L. Z.; Zhang, L. P.; Tung, C. H. *Chem. Phys. Lett.* **2002**, *356*, 573. (d) Fang, H.-H.; Chen, Q.-D.; Yang, J.; Xia, H.; Ma, Y.-G.; Wang, H.-Y.; Sun, H.-B. *Opt. Lett.* **2010**, *35*, 441.
- (19) (a) Jiang, Y.; Wang, Y.; Wang, B.; Yang, J.; He, N.; Qian, S.; Hua, J. *Chem. Asian J.* **2011**, *6*, 157. (b) He, G. S.; Lin, T. C.; Prasad, P. N.; Cho, C. C.; Yu, L. *J. Appl. Phys. Lett.* **2003**, *82*, 4717.
- (20) (a) Parthenopoulos, D. A.; Rentzepis, P. M. *Science* **1989**, *245*, 843. (b) Strickler, J. H.; Webb, W. W. *Opt. Lett.* **1991**, *16*, 1780. (c) Belfield, K. D.; Schafer, K. J. *Chem. Mater.* **2002**, *14*, 3656. (d) Belfield, K. D.; Liu, Y.; Negres, R. A.; Fan, M.; Pan, G.; Hagan, D. J.; Hernandez, F. E. *Chem. Mater.* **2002**, *14*, 3663.
- (21) (a) Tao, S.; Li, L.; Yu, J.; Jiang, Y.; Zhou, Y.; Lee, C.-S.; Lee, S.-T.; Zhang, X.; Kwon, O. *Chem. Mater.* **2009**, *21*, 1284. (b) Patra, A.; Pan, M.; Friend, C. S.; Lin, T.-C.; Cartwright, A. N.; Prasad, P. N.; Burzynski, R. *Chem. Mater.* **2002**, *14*, 4044. (c) Hancock, J. M.; Gifford, A. P.; Zhu, Y.; Lou, Y.; Jenekhe, S. A. *Chem. Mater.* **2006**, *18*, 4924. (d) Kulkarni, A. P.; Zhu, Y.; Babel, A.; Wu, P.-T.; Jenekhe, S. A. *Chem. Mater.* **2008**, *20*, 4212. (e) Thomas, K. R. J.; Lin, J. T.; Tao, Y.-T.; Chuen, C.-H. *Chem. Mater.* **2002**, *14*, 3852. (f) Huang, J.; Su, J.-H.; Li, X.; Lam, M.-K.; Fung, K.-M.; Fan, H.-H.; Kok-Wai Cheah, K.-W.; Chen, C. H.; Tian, H. *J. Mater. Chem.* **2011**, *21*, 2957.
- (22) Lee, W.-Y.; Wang, T.-F.; Chueh, C.-C.; Chen, W.-C.; Tuan, C.-S.; Lin, J.-J. *Macromol. Chem. Phys.* **2007**, *208*, 1919.
- (23) (a) Birks, J. B. *Photophysics of Aromatic Molecules*; Wiley: London, U.K., 1970. (b) Copek, I. *Adv. Colloid Interface Sci.* **2002**, *97*, 91. (c) Mancin, F.; Scrimin, P.; Tecilla, P.; Tonellato, U. *Coord. Chem. Rev.* **2009**, *293*, 2150.
- (24) (a) Thomas, S. W., III; Joly, G. D.; Swager, T. M. *Chem. Rev.* **2007**, *107*, 1339. (b) Shih, P.-I.; Chiang, C.-L.; Dixit, A. K.; Chen, C.-K.; Yuan, M.-C.; Lee, R.-Y.; Chen, C.-T.; Diau, E. W.-G.; Shu, C.-F. *Org. Lett.* **2006**, *8*, 2799. (c) Chen, C.-T. *Chem. Mater.* **2004**, *16*, 4389.
- (25) (a) Swager, T. M. *Acc. Chem. Res.* **2008**, *41*, 1181. (b) Grimsdale, A. C.; Chan, K. L.; Martin, R. E.; Jokisz, P. G.; Holmes, A. B. *Chem. Rev.* **2009**, *109*, 897. (c) Lee, S. H.; Jang, B. B.; Kafafi, Z. H. *J. Am. Chem. Soc.* **2005**, *127*, 9071. (d) Marsitzky, D.; Vestberg, R.; Blainey, P.; Tang, B. T.; Hawker, C. J.; Carter, K. R. *J. Am. Chem. Soc.* **2001**, *123*, 6965. (e) Setayesh, S.; Grimsdale, A. C.; Weil, T.; Enkelmann, V.; Muellen, K.; Meghdadi, F.; List, E. J. W.; Leising, G. *J. Am. Chem. Soc.* **2001**, *123*, 946. (f) Chiang, C.-L.; Tseng, S.-M.; Chen, C.-T.; Hsu, C.-P.; Shu, C.-F. *Adv. Funct. Mater.* **2008**, *18*, 248. (g) Hecht, S.; Frechet, J. M. *J. Angew. Chem., Int. Ed.* **2001**, *40*, 74. (h) Tang, C. W.; Vanslyke, S. A.; Chen, C. H. *J. Appl. Phys.* **1989**, *65*, 3610. (i) Bulovic, V.; Shoustikov, A.; Baldo, M. A.; Bose, E.; Kozlov, V. G.; Thompson, M. E.; Forrest, S. R. *Chem. Phys. Lett.* **1998**, *287*, 455. (j) Xia, Z.-Y.; Su, J.-H.; Fan, H.-H.; Cheah, K.-W.; Tian, H.; Chen, C. H. *J. Phys. Chem. C* **2010**, *114*, 11602.
- (26) (a) Luo, J.; Xie, Z.; Lam, J. W. Y.; Cheng, L.; Chen, H.; Qiu, C.; Kwok, H. S.; Zhan, X.; Liu, Y.; Zhu, D.; Tang, B. Z. *Chem. Commun.* **2001**, 1740. (b) Hong, Y.; Lam, J. W. Y.; Tang, B. Z. *Chem. Commun.* **2009**, 4332. (c) Hong, Y.; Lam, J. W. Y.; Tang, B. Z. *Chem. Soc. Rev.* **2011**, *40*, 5361. (d) Zhao, Z.; Lam, J. W. Y.; Tang, B. Z. *Curr. Org. Chem.* **2010**, *14*, 2109. (e) Yuan, W. Z.; Zhao, H.; Shen, X. Y.; Mahtab, F.; Lam, J. W. Y.; Sun, J. Z.; Tang, B. Z. *Macromolecules* **2009**, *42*, 9400.
- (27) (a) Zhao, Z.; Wang, Z.; Lu, P.; Chan, C. Y. K.; Liu, D.; Lam, J. W. Y.; Sung, H. H. Y.; Williams, I. D.; Ma, Y.; Tang, B. Z. *Angew. Chem., Int. Ed.* **2009**, *48*, 7608. (b) Yuan, W. Z.; Lu, P.; Chen, S.; Lam, J. W. Y.; Wang, Z.; Liu, Y.; Kowk, H. S.; Ma, Y.; Tang, B. Z. *Adv. Mater.* **2010**, *22*, 2159. (c) Zeng, Q.; Li, Z.; Dong, Y.; Di, C.; Qin, A.; Hong, Y.; Ji, L.; Zhu, Z.; Jim, C. K. W.; Yu, G.; Li, Q.; Li, Z.; Liu, Y.; Qin, J.; Tang, B. Z. *Chem. Commun.* **2007**, *70*. (d) Dong, S.; Li, Z.; Qin, J. *J. Phys. Chem. B* **2009**, *113*, 434. (e) Yuan, W. Z.; Chen, S.; Lam, J. W. Y.; Deng, C.; Lu, P.; Sung, H. H.-Y.; Williams, I. D.; Kwok, H. S.; Zhang, Y.; Tang, B. Z. *Chem. Commun.* **2011**, *47*, 11216. (f) Yuan, W. Z.; Yu, Z.-Q.; Tang, Y.; Lam, J. W. Y.; Xie, N.; Lu, P.; Chen, E.-Q.; Tang, B. Z. *Macromolecules* **2011**, *44*, 9618.
- (28) (a) Yuan, W. Z.; Mahtab, F.; Gong, Y.; Yu, Z.; Lu, P.; Tang, Y.; Lam, J. W. Y.; Zhu, C.; Tang, B. Z. *J. Mater. Chem.* **2012**, DOI: 10.1039/c2jm30620d. (b) Yang, Z.; Chi, Z.; Yu, T.; Zhang, X.; Chen, M.; Xu, B.; Liu, S.; Zhang, Y.; Xu, J. *J. Mater. Chem.* **2009**, *19*, 5541. (c) An, B.-K.; Gilhm, S. H.; Chung, J. W.; Park, C. R.; Kwon, S.-K.; Park, S. Y. *J. Am. Chem. Soc.* **2009**, *131*, 3950. (d) Yoon, S.-J.; Park, S. Y. *J. Mater. Chem.* **2011**, *21*, 8338. (e) Wang, M.; Zhang, G.; Zhang, D.; Zhu, D.; Tang, B. Z. *J. Mater. Chem.* **2010**, *20*, 1858. (f) Wang, M.; Zhang, D.; Zhang, G. X.; Zhu, D. B. *Chem. Commun.* **2008**, 4469. (g) Han, T.; Feng, X.; Tong, B.; Shi, J.; Chen, L.; Zhi, J.; Dong, Y. *Chem. Commun.* **2012**, *48*, 416. (h) Yuan, W. Z.; Yu, Z.-Q.; Lu, P.; Deng, C.; Lam, J. W. Y.; Wang, Z.; Chen, E.-Q.; Ma, Y.; Tang, B. Z. *J. Mater. Chem.* **2012**, *22*, 3323. (i) Yuan, W. Z.; Shen, X. Y.; Zhao, H.; Lam, J. W. Y.; Tang, L.; Lu, P.; Wang, C.; Liu, Y.; Wang, Z.; Zheng, Q.; Sun, J. Z.; Ma, Y.; Tang, B. Z. *Phys. Chem. C* **2010**, *114*, 6090.
- (29) (a) Lakowicz, J. R. *Principles of Fluorescence Spectroscopy*, 3rd ed.; Springer: New York, U.S.A., 2006; Chapter 6, pp 205–235. (b) Jones, G., II; Jackson, W. R.; Choi, C. Y.; Bergmark, W. R. *J. Phys. Chem.* **1985**, *89*, 294. (c) Kosower, E. M.; Dodiuk, H.; Kanety, H. *J. Am. Chem. Soc.* **1978**, *100*, 4179.
- (30) (a) Palayangoda, S. S.; Cai, X.; Adhikari, R. M.; Neckers, D. C. *Org. Lett.* **2008**, *10*, 281. (b) Liu, Y.; Tao, X.; Wang, F.; Dang, X.; Zou, D.; Ren, Y.; Jiang, M. *J. Phys. Chem. C* **2008**, *112*, 3975. (c) Xu, J.; Liu, X.; Lv, J.; Zhu, M.; Huang, C.; Zhou, W.; Yin, X.; Liu, H.; Li, Y.; Ye, J. *Langmuir* **2008**, *24*, 4231. (d) Yeh, H.-C.; Yeh, S.-J.; Chen, C.-T. *Chem. Commun.* **2003**, 2632.
- (31) (a) Gao, B.-R.; Wang, H.-Y.; Yang, Z.-Y.; Wang, H.; Wang, L.; Jiang, Y.; Hao, Y.-W.; Chen, Q.-D.; Li, Y.-P.; Ma, Y.-G.; Sun, H.-B. *J. Phys. Chem. C* **2011**, *115*, 16150. (b) Gao, B.-R.; Wang, H.-Y.; Hao, Y.-W.; Fu, L.-M.; Fang, H.-H.; Jiang, Y.; Wang, L.; Chen, Q.-D.; Xia, H.; Pan, L.-Y.; Ma, Y.-G.; Sun, H.-B. *J. Phys. Chem. B* **2010**, *114*, 128.
- (32) (a) Peng, X.; Song, F.; Lu, E.; Wang, Y.; Zhou, W.; Fan, J.; Gao, Y. *J. Am. Chem. Soc.* **2005**, *127*, 4170. (b) Zaheer, A.; Lenkinski, R. E.; Mahmood, A.; Jones, A. G.; Cantley, L. C.; Frangioni, J. V. *Nat. Biotechnol.* **2001**, *19*, 1148.
- (33) Häussler, M.; Liu, J.; Zheng, R.; Lam, J. W. Y.; Qin, A.; Tang, B. Z. *Macromolecules* **2007**, *40*, 1914.
- (34) (a) Wang, S.; Oldham, W. J., Jr.; Hudack, R. A., Jr.; Bazan, G. C. *J. Am. Chem. Soc.* **2000**, *122*, 5695. (b) Gilbert, J.; Miquel, J.-F.; Précigoux, G.; Haospital, M.; Raynaud, J.-P.; Michel, F.; de Paulet, A. C. *J. Med. Chem.* **1983**, *26*, 693.
- (35) (a) Lippert, E. Z. *Naturforsch. A: Phys. Sci.* **1955**, *10*, 541. (b) Mataga, N.; Kaifu, Y.; Koizumi, M. *Bull. Chem. Soc. Jpn.* **1956**, *29*, 465.
- (36) Hu, R.; Lager, E.; Aguilar-Aguilar, A.; Liu, J.; Lam, J. W. Y.; Sung, H. H.-Y.; Williams, I. D.; Zhong, Y.; Wong, K. S.; Peña-Cabrera, E.; Tang, B. Z. *J. Phys. Chem. C* **2009**, *113*, 15845.
- (37) Addition of water into THF increases the solvent polarity and decreases the solvating power. The former decreases the emission intensity of an ICT luminogen, whereas the latter promotes aggregate formation and activates the AIE process. The emission of TPA3TPAN and DTPA4TPAN molecules is thus determined by the competition between these two antagonistic effects.

- (38) (a) Ko, C.-W.; Tao, Y.-T. *Synth. Met.* **2002**, *126*, 37. (b) Naito, K.; Miura, A. *J. Phys. Chem.* **1993**, *97*, 6240. (c) Ham, E.; Do, L.; Niidome, Y.; Fujihira, M. *Chem. Lett.* **1994**, 969.
- (39) (a) Zhao, H.; Tanjutco, C.; Thayumanavan, S. *Tetrahedron Lett.* **2001**, *42*, 4421. (b) Low, P. J.; Paterson, M. A. J.; Yusfit, D. S.; Howard, J. A. K.; Cherryman, J. C.; Tackley, D. R.; Brook, R.; Brow, B. *J. Mater. Chem.* **2005**, *15*, 2304.
- (40) Liu, Y.; Chen, S.; Lam, J. W. Y.; Lu, P.; Kwok, R. T. K.; Mahtab, F.; Kwok, H. S.; Tang, B. Z. *Chem. Mater.* **2011**, *23*, 2536.
- (41) (a) Tao, S. L.; Lee, C. S.; Lee, S. T.; Zhang, X. H. *Appl. Phys. Lett.* **2007**, *91*, 013507. (b) Tong, Q.-X.; Lai, S.-L.; Chan, M.-Y.; Zhou, Y.-C.; Kwong, H.-L.; Lee, C.-S.; Lee, S.-T. *Chem. Mater.* **2008**, *20*, 6310.
- (42) (a) Yan, H.; Huang, Q.; Cui, J.; Veinot, J. G. C.; Kern, M. M.; Marks, T. J. *Adv. Mater.* **2003**, *15*, 835. (b) Chin, B. D.; Suh, M. C.; Lee, S. T.; Chung, H. K.; Lee, C. H. *Appl. Phys. Lett.* **2004**, *84*, 1777. (c) Veinot, J. G. C.; Marks, T. J. *Acc. Chem. Res.* **2005**, *38*, 632.